2. Horwitz LD, Kaufman D, Keller MW, Kong Y. Time course of coronary endothelial healing after injury due to ischemia and reperfusion. Circulation 1994;90:2439–47.
3. Dauber IM, Van Benthuysen KM, McMurtry IF, et al. Functional coronary microvascular injury evident as increased permeability due to brief ischemia and reperfusion. Circ Res 1990;66:986–98.
4. Forman MB, Stone GW, Jackson EK. Role of adenosine as adjunctive therapy in acute myocardial infarction. Cardiovasc Drug Rev 2006;24:116–47.
5. Mubagwa K, Flameng W. Adenosine, adenosine receptors and myocardial protection: an updated overview. Cardiovasc Res 2001;52:25–39.
6. Mahaffey KW, Pume JA, Barbagelata NA, et al. Adenosine as an adjunct to thrombolytic therapy for acute myocardial infarction: results of a multicenter, randomized, placebo-controlled trial: the Acute Myocardial Infarction STudy of ADenosine (AMISTAD) trial. J Am Coll Cardiol 1999;34:1711–20.
7. Ross AM, Gibbons RJ, Stone GW, Kloner RA, Alexander RW, for the AMISTAD-II ÅInvestigators. A randomized, double-blinded, placebo-controlled multicenter trial of adenosine as an adjunct to reperfusion in the treatment of acute myocardial infarction (AMISTAD-II). J Am Coll Cardiol 2005;45:1775–80.
8. Bullard AJ, Govewalla P, Yellon DM. Erythropoietin protects the myocardium against reperfusion injury in vitro and in vivo. Basic Res Cardiol 2005;100:397–403.
9. Hannon JP, Tigani B, Wolber C, et al. Evidence for an atypical receptor mediating the augmented bronchoconstrictor response to adenosine induced by allergen challenge in activity sensitized Brown Norway rats. Br J Pharmacol 2002;135:685–96.
10. Kin H, Zatta AJ, Lofye MT, et al. Postconditioning reduces infarct size via adenosine receptor activation by endogenous adenosine. Cardiovasc Res 2005;67:124–33.
11. Hinschen AK, RoseMeyer RB, Headrick JP. Adenosine receptor subtypes mediating coronary vasodilation in rat hearts. J Cardiovasc Pharmacol 2003;41:73–80.
12. Kaeffeer N, Richard V, Francois A, Lallemand F, Henry JP, Thuillez C. Preconditioning prevents chronic reperfusion-induced coronary endothelial dysfunction in rats. Am J Physiol 1996;271:H842–9.
13. M Shimizu, Miwa K, Hashimoto Y, Goto A. Encapsulating of chicken egg yolk immunoglobulin G (IgY) by liposomes. Biosci Biotechnol Biochem 1993;57:1445–9.
14. Kasuya T, Jung J, Kadoya H, et al. In vivo delivery of bionanocapsules displaying phaseolus vulgaris agglutinin-L(4) isolectin to malignant tumors overexpressing N-acetylglucosaminlyltransferase V. Hum Gene Ther 2008;19:887–95.
15. Kim YD, Fomsgaard JS, Heim KF, et al. Brief ischemia-reperfusion induces stunning of endothelium in canine coronary artery. Circulation 1992;85:1473–82.
16. Canyon SJ, Dobson GP. Protection against ventricular arrhythmias and cardiac death using adenosine and lidocaine during regional ischemia in the in vivo rat. Am J Physiol Heart Circ Physiol 2004;287:H1286–95.
17. Yaar R, Jones MR, Chen JF, Ravid K. Animal models for the study of adenosineÅreceptor function. J Cell Physiol 2005;202:9–20.
18. Norton ED, Jackson EK, Turner MB, Virmani R, Forman MB. The effects of intravenous infusions of selective adenosine A_1-receptor and A_2-receptor agonists on myocardial reperfusion injury. Am Heart J 1992;123:332–8.
19. Xu Z, Mueller RA, Park SS, Boysen PG, Cohen MV, Downey JM. Cardioprotection with adenosine A_2 receptor activation at reperfusion. J Cardiovasc Pharmacol 2005;46:794–802.
20. Vinten-Johansen J. Postconditioning: a mechanical maneuver that triggers biological and molecular cardioprotective responses to reperfusion. Heart Fail Rev 2007;12:235–344.
21. Lasic DD. Doxorubicin in sterically stabilized liposomes. Nature 1996;380:561–2.

Key Words: myocardial infarction ▪ liposome ▪ drug delivery system ▪ adenosine.

Noninvasive Estimation of Pulmonary Vascular Resistance by Doppler Echocardiography in Patients With Pulmonary Arterial Hypertension

Hidemichi Kouzu, MD[a], Satoshi Nakatani, MD, PhD[a,*], Shingo Kyotani, MD, PhD[a], Hideaki Kanzaki, MD[a], Norifumi Nakanishi, MD, PhD[a], and Masafumi Kitakaze, MD, PhD[a]

Pulmonary vascular resistance (PVR) is an important hemodynamic variable in the management of patients with pulmonary hypertension. To establish a method of estimating PVR in patients with pulmonary arterial hypertension (PAH), Doppler echocardiography was performed within 24 hours of right heart catheterization in 43 patients with PAH (idiopathic PAH, n = 20; chronic thromboembolic pulmonary hypertension, n = 9; congenital heart disease, n = 9; and others). Correlations between invasive PVR and Doppler variables of pulmonary artery flow and tricuspid regurgitation were examined. Mean invasive PVR was 1,294 ± 680 dyne s cm^{-5}. Linear regression analysis revealed significant correlations with invasive PVR for the time–velocity integral (TVI; r = −0.63, p = 0.009) of right ventricular outflow and peak tricuspid regurgitant pressure gradient (TRPG; r = 0.77, p <0.001). The TRPG/TVI ratio, which approximated the ratio of pulmonary artery pressure to pulmonary blood flow, showed an improved correlation coefficient of 0.82 (PVR = 187 + TRPG/TVI × 118, p <0.001). After excluding 5 patients with an intracardiac shunt, 26 of the remaining 38 patients (68%) met the hemodynamic criteria in international guidelines for the selection of lung transplantation candidates and were defined as the poor-prognosis group. A TRPG/TVI >7.6 showed 85% sensitivity and 92% specificity for identifying patients in the poor-prognosis group. In conclusion, TRPG/TVI provides a reliable estimation of PVR over a wide range in patients with PAH with various underlying causes. © 2009 Elsevier Inc. (Am J Cardiol 2009;103:872–876)

Doppler echocardiography provides a simple and noninvasive means of assessing hemodynamics in patients with pulmonary arterial hypertension (PAH). Although the peak tricuspid regurgitant pressure gradient (TRPG) calculated from Doppler-derived tricuspid regurgitation velocity is the most useful and practical method for estimating pulmonary artery pressure,[1] it has shown no predictive value in previous studies.[2–5] Because cardiac output has been shown to be independently predictive,[6] assessment of pulmonary vascular resistance (PVR), which includes not only pulmonary artery pressure but also cardiac output in the equation, is of great importance in evaluating the severity of PAH. Recent reports have demonstrated that the ratio of tricuspid regurgitation velocity to the time–velocity integral (TVI) of the right ventricular outflow tract (RVOT) correlates well with PVR.[7,8] The methods in those studies, however, were not fully validated in patients with PAH. This study examined whether TRPG/TVI can provide a reliable estimation of PVR in patients with PAH with various underlying causes and clarify a suitable cut-off value for selecting patients with a potentially poor prognosis.

Methods

Subjects were 43 patients with sinus rhythm and pulmonary hypertension. Patients with left-side heart disease were excluded. Each patient provided written informed consent before participation in the study. Doppler echocardiography was performed within 24 hours of catheterization. Measurements were performed with an observer blinded to cardiac catheterization data. No changes were made to medication between catheterization and Doppler echocardiographic procedures and oxygen therapy was withheld during each examination.

A Sonos 5500 ultrasound system equipped with an S4 transducer (Hewlett-Packard, Andover, Massachusetts) was used. Echocardiographic studies were performed in the left lateral decubitus or supine position. The systolic pattern of pulmonary artery flow was obtained by placing a pulse-wave Doppler sample volume just below the pulmonary valve in the parasternal short-axis view. The following variables were measured: maximal systolic flow velocity; TVI; acceleration time, expressed as the interval between onset of ejection and time of peak flow velocity; and ejection time, expressed as the interval between onset and end of systolic flow velocity recording. Continuous-wave Doppler was used to determine peak tricuspid regurgitation velocity. Several views were used to obtain the best possible alignment between regurgitation flow and the Doppler ultrasound beam. TRPG was calculated by applying the simplified Bernoulli equation. According to a previous report,[9] functional pre-ejection period was defined as the interval be-

[a]Division of Cardiology, Department of Internal Medicine, National Cardiovascular Center, Osaka, Japan.; Manuscript received September 6, 2008; revised manuscript received and accepted November 15, 2008.

*Corresponding author: Tel/fax: 81-6-6879-2561.
E-mail address: nakatani@sahs.med.osaka-u.ac.jp (S. Nakatani).

0002-9149/09/$ – see front matter © 2009 Elsevier Inc.
doi:10.1016/j.amjcard.2008.11.039

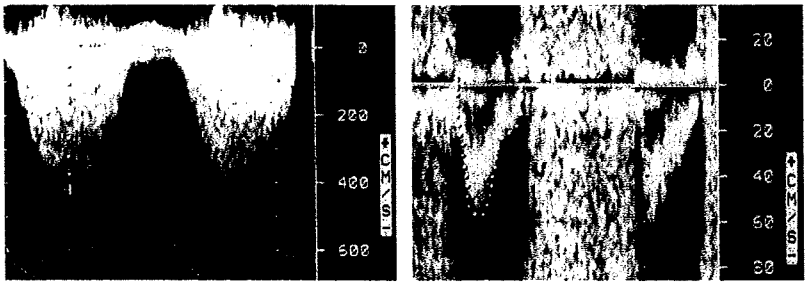

Figure 1. Images showing TRPG *(left)* and TVI of the RVOT *(right)* in a patient with idiopathic PAH (TRPG 74.4 mm Hg, TVI 8.6 cm, TRPG 74.4/TVI 8.6 = 8.7). This patient's invasive PVR was 1,426 dyne s cm^{-5}.

tween onset of tricuspid regurgitation and onset of systolic pulmonary artery flow, and total systolic time was defined as the sum of pre-ejection period and ejection time. An average of ≥5 beats was analyzed, and then TRPG/TVI was calculated (Figure 1).

A Swan-Ganz catheter was used for hemodynamic measurements. Pulmonary capillary wedge pressure, pulmonary artery mean pressure, and right atrial pressure were measured. Transpulmonary flow was calculated using the estimated Fick principle. PVR (expressed in dyne s cm^{-5}) was calculated using the following formula: PVR = 80 × (pulmonary artery mean pressure − pulmonary capillary wedge pressure)/transpulmonary flow.

Continuous variables were expressed as means ± SDs. Student's *t* test was used to compare continuous variables. The relation between catheter measurements and Doppler echocardiography was assessed by linear regression and Bland-Altman analyses.[10] Stepwise regression analysis was used to evaluate the predictive power of independent variables. A p value <0.05 was considered statistically significant. A receiver operating characteristic curve was generated to determine a poor-prognosis group, and a cut-off value was obtained for TRPG/TVI with balanced sensitivity and specificity values. Intraobserver and interobserver variabilities described by the coefficient of variation were assessed on the same recording in 10 randomly selected subjects. Measurements for interobserver variability were performed by 2 independent investigators who had performed Doppler echocardiography for ≥2 years. All statistical analyses were performed using JMP 7.0 (SAS Institute, Cary, North Carolina).

Results

Patient characteristics and invasive hemodynamic and Doppler echocardiographic data are presented in Tables 1 and 2. Heart rate was similar during cardiac catheterization (82 ± 17 beats/min) and echocardiography (81 ± 13 beats/min, p = 0.81). Correlations between Doppler flow velocity variables and PVR are presented in Table 3. Maximal systolic flow velocity, ejection time, and acceleration time index, defined as the ratio of acceleration time to ejection time, showed weak correlations with PVR. Acceleration time and TVI showed modest negative correlations with PVR, whereas TRPG showed the strongest correlation with PVR. In stepwise regression analysis, only TVI and TRPG showed significant results. When the correlation between TRPG/TVI and PVR was examined, an improved correlation coefficient of 0.82 was revealed (Figure 2). This correlation remained robust in all patient groups. In Bland-Altman analysis, the mean relative difference between measured PVR and estimated PVR was close to 0 for the entire population, indicating the absence of any systematic error (Figure 2).

Table 1
Clinical and demographic characteristics of patients (n = 43)

Characteristics	Findings
Men/women	12/31
Mean age (yrs) (range)	44 (14–72)
Diagnosis	
Idiopathic PAH	20
Chronic thromboembolic pulmonary hypertension	9
Congenital heart disease (after repair)	9 (44%)
Collagen vascular disease	3
Other	2

Table 2
Hemodynamic and Doppler echocardiographic characteristics

	Mean ± SD	Range
Invasive hemodynamics		
Heart rate (beats/min)	82 ± 17	50–120
Mean arterial pressure (mm Hg)	84 ± 9	66–102
Pulmonary capillary wedge pressure (mm Hg)	8 ± 3	2–17
Pulmonary artery mean pressure (mm Hg)	55 ± 17	21–90
Right atrial pressure (mm Hg)	6 ± 4	0–14
PVR (dyne s cm^{-5})	1,294 ± 680	93–3,113
Doppler pulmonary artery flow		
Maximal systolic velocity (cm/s)	66 ± 20	29–138
TVI (cm)	11.1 ± 3.9	5.7–24.3
Pre-ejection time (ms)	50 ± 21	0–90
Acceleration time (ms)	78 ± 24	42–150
Ejection time (ms)	269 ± 44	154–354
Total systolic time (ms)	319 ± 43	203–388
Acceleration time index	0.29 ± 0.08	0.12–0.51
Tricuspid regurgitation flow		
TRPG (mm Hg)	90 ± 30	35–154

According to international guidelines for the selection of lung transplantation candidates, useful hemodynamic parameters for assessing the failure of optimal pretransplantation therapy in patients with pulmonary hypertension but without congenital shunts include a cardiac index <2 L/min/m^2, a right atrial pressure >15 mm Hg, and a pulmonary artery mean pressure >55 mm Hg.[11] These 3 he-

Table 3
Correlations between Doppler variables and pulmonary vascular resistance

	Correlation Coefficient	p Value	
		Univariate	Multivariate
Maximal systolic velocity	−0.42	0.006	0.82
TVI	−0.63	<0.001	0.009
Pre-ejection time	0.21	0.18	0.39
Acceleration time	−0.59	<0.001	0.69
Ejection time	−0.37	0.01	0.95
Total systolic time	−0.30	0.05	0.73
Acceleration time index	−0.42	0.005	—
TRPG	0.77	<0.001	<0.001

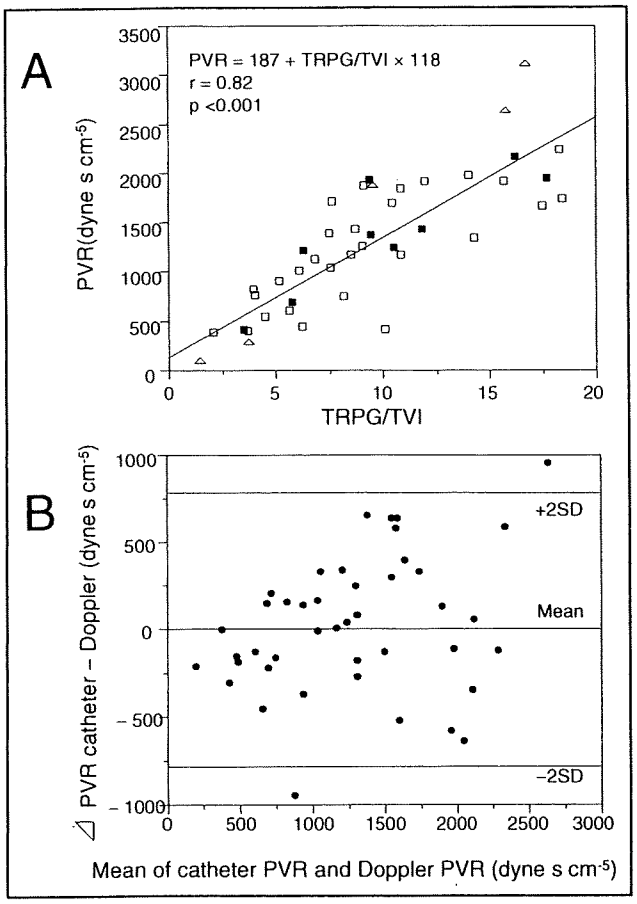

Figure 2. *(A)* Linear regression analysis between PVR and TRPG/TVI. Patients with chronic thromboembolic pulmonary hypertension *(solid squares)*, intracardiac shunts *(triangles)*, and others *(open squares)* were evenly distributed in the study population. *(B)* Bland-Altman plot shows the mean difference *(solid line)* ± 2 SDs *(dotted line)* between catheter PVR and Doppler PVR.

modynamic variables independently correlate well with mortality.[6] In our study population excluding 5 patients with intracardiac shunts, 26 patients (68%) met ≥1 of these criteria and were defined as the poor-prognosis group. Mean PVR was significantly higher in the poor-prognosis group than in the remaining 12 patients (1,522 ± 434 vs 675 ± 283 dyne s cm^{-5}, p <0.001). Using receiver operating characteristic analysis, a TRPG/TVI cut-off value of 7.6

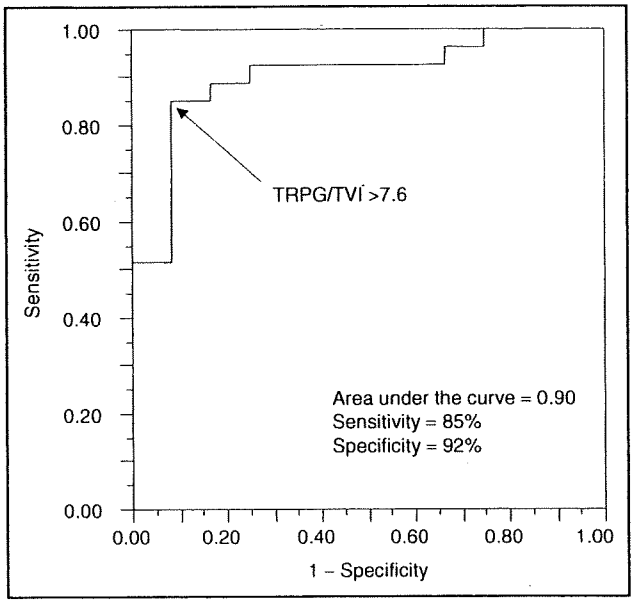

Figure 3. Receiver operating characteristic curve to identify patients with a poor prognosis.

showed 85% sensitivity and 92% specificity for identifying patients with a poor prognosis (area under the curve 0.90; Figure 3).

Intraobserver and interobserver variabilities were good for TVI (5.9% and 9.5%, respectively) and TRPG (5.7% and 8.8%, respectively).

Discussion

The major findings in this study were that (1) TRPG/TVI provides a reliable estimation of PVR over a wide range in PAH of various underlying causes, including intracardiac shunt diseases, and (2) TRPG/TVI >7.6 suggests poor prognosis for patients with PAH without an intracardiac shunt.

Various Doppler parameters have been used to evaluate PVR. In previous studies, attention was focused on pulmonary artery flow morphologic patterns, but correlations with PVR were weak.[12,13] Scapellato et al[9] reported that pre-ejection period/acceleration time ratio, normalized for total systolic time, correlated well with PVR. However, their study population did not include patients with PAH. Selimovic et al[14] reported that comprehensive hemodynamic assessment by Doppler echocardiography can provide an accurate estimation of PVR by dividing the transpulmonary pressure gradient by cardiac output in patients with PAH. However, that method requires laborious techniques that are not routinely used.

PVR is calculated invasively as the ratio of transpulmonary pressure gradient to transpulmonary flow.[15] The closest noninvasive representative parameters of these values are TRPG and TVI of the RVOT, respectively.[16,17] As PVR increases, TRPG increases and TVI decreases.[17,18] Abbas et al[7] reported that the ratio of peak tricuspid regurgitation velocity to TVI correlated well with PVR. This method is simple and reliable but has been validated only in a small number of patients with PAH.[8] The present study demon-

strates that our method appears applicable to patients with PAH with various underlying causes.

Hemodynamic parameters for the selection of lung transplantation candidates are based on prognosis in the era of conventional therapy.[6,11] Those hemodynamic parameters are predictive if a patient is left untreated. Over the previous decade, advances in medical therapies with a prostanoid, endothelin receptor antagonist, or phosphodiesterase-5 inhibitor have changed the clinical course of PAH.[19–21] Baseline hemodynamic variables thus appear to be less prognostic. However, the prognosis of patients refractory to these optimal medical therapies remains poor and lung transplantation should be considered in such cases. Our Doppler index may be useful in assessing response to therapy, and the cut-off value may be predictive and helpful in considering lung transplantation as a therapeutic option if a patient is fully medicated. Pulmonary hypertension in patients with congenital heart defects shows different a prognosis compared with other types of pulmonary hypertension. Similar pulmonary artery pressure is generally associated with a higher cardiac index, a lower right atrial pressure, and a somewhat better prognosis in these patients.[22] Conversely, because prognosis in patients with a previously repaired heart defect and severe pulmonary hypertension resembles that of patients with idiopathic PAH,[22] these patients can be treated in a similar manner to patients with idiopathic PAH.

In routine echocardiographic examination of patients with PAH, we measure TRPG to estimate pulmonary artery pressure. However, it has not shown any predictive value in previous studies.[2–5] In addition, the first hemodynamic change in patients with PAH who respond to vasodilator pharmacotherapy is a decrease in PVR and an increase in cardiac output, whereas pulmonary artery pressure does not change significantly.[23] In such situations, assessment of TRPG alone may underestimate the hemodynamic response to vasodilators. TRPG/TVI thus offers a superior index to TRPG alone, because this measurement includes the parameter of cardiac output in the equation. Accurate noninvasive estimation of PVR by TRPG/TVI would decrease the need for invasive right heart catheterization. TRPG/TVI may be also helpful in patients with intracardiac shunt, to distinguish between hyperdynamic flow states and true pulmonary vascular disease and to determine indications for defect repair.

Several limitations of the present study should be considered. First, invasive and noninvasive measurements were not performed simultaneously in the present study. However, simultaneous measurements of echocardiography may become inaccurate due to suboptimal positioning of the patient. The delay within 24 hours between echocardiography and catheterization was acceptable.[8,14] Second, proper alignment of the ultrasound beam is crucial to ensure adequate determination of TRPG and TVI. Fine adjustment of the probe angle was required to obtain the highest velocity. We used the modified Bernoulli equation, which might cause some errors when the tricuspid origin is grossly dilated. Furthermore, potentially a severe jet of tricuspid regurgitation and increased right atrial pressure would produce a low TRPG even in the presence of marked pulmonary hypertension.[17] However, in our subjects, TRPG showed a strong correlation with pulmonary artery pressure ($r = 0.85$, $p < 0.001$, data not shown) despite a wide range of right atrial pressure. Third, estimation of PVR by TRPG/TVI does not account for some potentially confounding hemodynamic variables and anatomic variations including pulmonary capillary wedge pressure, heart rate, and RVOT diameter. However, in patients with PAH, transpulmonary pressure gradient should be mostly proportional to TRPG because wide variations in pulmonary capillary wedge pressure are not typically seen. Furthermore, measurement of RVOT diameter is not practical because the edge of the dilated RVOT often cannot be recognized. We thus used TVI as a representative parameter of transpulmonary flow without correcting for RVOT diameter, which was performed in a previous study.[8] We examined the effect of correcting TVI for heart rate on estimation of PVR by dividing TVI by 1 cardiac cycle length. The correlation between TRPG/TVI for heart rate and PVR did not improve (data not shown). Simplification by neglecting heart rate is thus acceptable. Fourth, more patients with an intracardiac shunt should be examined, given the small number of such patients in our study. Fifth, because our study population included a wide range of patients, from untreated to those treated with intravenous epoprostenol, a simple comparison of actual prognoses was not performed. Further studies are needed to validate our cut-off value in fully medicated patients.

1. Chan KL, Currie PJ, Seward JB, Hagler DJ, Mair DD, Tajik AJ. Comparison of three Doppler ultrasound methods in the prediction of pulmonary artery pressure. *J Am Coll Cardiol* 1987;9:549–554.
2. Eysmann SB, Palevsky HI, Reichek N, Hackney K, Douglas PS. Two-dimensional and Doppler-echocardiographic and cardiac catheterization correlates of survival in primary pulmonary hypertension. *Circulation* 1989;80:353–360.
3. Yeo TC, Dujardin KS, Tei C, Mahoney DW, McGoon MD, Seward JB. Value of a Doppler-derived index combining systolic and diastolic time intervals in predicting outcome in primary pulmonary hypertension. *Am J Cardiol* 1998;81:1157–1161.
4. Raymond RJ, Hinderliter AL, Willis PW, Ralph D, Caldwell EJ, Williams W, Ettinger NA, Hill NS, Summer WR, de Boisblanc B, et al. Echocardiographic predictors of adverse outcomes in primary pulmonary hypertension. *J Am Coll Cardiol* 2002;39:1214–1219.
5. Mori S, Nakatani S, Kanzaki H, Yamagata K, Take Y, Matsuura Y, Kyotani S, Nakanishi N, Kitakaze M. Patterns of the interventricular septal motion can predict conditions of patients with pulmonary hypertension. *J Am Soc Echocardiogr* 2008;21:386–393.
6. D'Alonzo GE, Barst RJ, Ayres SM, Bergofsky EH, Brundage BH, Detre KM, Fishman AP, Goldring RM, Groves BM, Kernis JT, et al. Survival in patients with primary pulmonary hypertension. Results from a national prospective registry. *Ann Intern Med* 1991;115:343–349.
7. Abbas AE, Fortuin FD, Schiller NB, Appleton CP, Moreno CA, Lester SJ. A simple method for noninvasive estimation of pulmonary vascular resistance. *J Am Coll Cardiol* 2003;41:1021–1027.
8. Vlahos AP, Feinstein JA, Schiller NB, Silverman NH. Extension of Doppler-derived echocardiographic measures of pulmonary vascular resistance to patients with moderate or severe pulmonary vascular disease. *J Am Soc Echocardiogr* 2008;21:711–714.
9. Scapellato F, Temporelli PL, Eleuteri E, Corrà U, Imparato A, Giannuzzi P. Accurate noninvasive estimation of pulmonary vascular resistance by Doppler echocardiography in patients with chronic failure heart failure. *J Am Coll Cardiol* 2001;37:1813–1819.
10. Bland JM, Altman DG. Statistical methods for assessing agreement between two methods of clinical measurement. *Lancet* 1986;327:307–310.
11. ASTP, ATS, ERS, ISHLT joint statement. International guidelines for the selection of lung transplant patients. *Am J Respir Crit Care Med* 1998;158:335–339.

12. Martin-Duran R, Larman M, Trugeda A, Vazquez de Prada JA, Ruano J, Torres A, Figueroa A, Pajaron A, Nistal F. Comparison of Doppler-determined elevated pulmonary arterial pressure with pressure measured at cardiac catheterization. *Am J Cardiol* 1986;57:859–863.
13. Dabestani A, Mahan G, Gardin JM, Takenaka K, Burn C, Allfie A, Henry WL. Evaluation of pulmonary artery pressure and resistance by pulsed Doppler echocardiography. *Am J Cardiol* 1987;59:662–668.
14. Selimovic N, Rundqvist B, Bergh CH, Andersson B, Petersson S, Johansson L, Bech-Hanssen O. Assessment of pulmonary vascular resistance by Doppler echocardiography in patients with pulmonary arterial hypertension. *J Heart Lung Transplant* 2007;26:927–934.
15. Willard JEL, Richard A, Hillis LD. Cardiac catheterization. In: Kloner RA, ed. The Guide to Cardiology, 3rd Ed. Greenwich, CT: Le Jacq Communications, 1995:151.
16. Ihlen H, Amlie JP, Dale J, Forfang K, Nitter-Hauge S, Otterstad JE, Simonsen S, Myhre E. Determination of cardiac output by Doppler echocardiography. *Br Heart J* 1984;51:54–60.
17. Yock PG, Popp RL. Noninvasive estimation of right ventricular systolic pressure by Doppler ultrasound in patients with tricuspid regurgitation. *Circulation* 1984;70:657–662.
18. Okamoto M, Miyatake K, Kinoshita N, Sakakibara H, Nimura Y. Analysis of blood flow in pulmonary hypertension with the pulsed Doppler flowmeter combined with cross sectional echocardiography. *Br Heart J* 1984;51:407–415.
19. Macchia A, Marchioli R, Marfisi R, Scarano M, Levantesi G, Tavazzi L, Tognoni G. A meta-analysis of trials of pulmonary hypertension: a clinical condition looking for drugs and research methodology. *Am Heart J* 2007;153:1037–1047.
20. Humbert M, Barst RJ, Robbins IM, Channick RN, Galiè N, Boonstra A, Rubin LJ, Horn EM, Manes A, Simonneau G. Combination of bosentan with epoprostenol in pulmonary arterial hypertension: BREATHE-2. *Eur Respir J* 2004;24:353–359.
21. Mathai SC, Girgis RE, Fisher MR, Champion HC, Housten-Harris T, Zaiman A, Hassoun PM. Addition of sildenafil to bosentan monotherapy in pulmonary arterial hypertension. *Eur Respir J* 2007;29:469–475.
22. Hopkins WE, Ochoa LL, Richardson GW, Trulock EP. Comparison of the hemodynamics and survival of adults with severe primary pulmonary hypertension or Eisenmenger syndrome. *J Heart Lung Transplant* 1996;15:100–105.
23. Sandoval J, Bauerle O, Palomar A, Gómez A, Martínez-Guerra ML, Beltrán M, Guerrero ML. Survival in primary pulmonary hypertension. Validation of a prognostic equation. *Circulation* 1994;89:1733–1744.

Journal of the American College of Cardiology
© 2009 by the American College of Cardiology Foundation
Published by Elsevier Inc.

Vol. 53, No. 22, 2009
ISSN 0735-1097/09/$36.00
doi:10.1016/j.jacc.2009.02.038

Natriuretic Peptides Enhance the Production of Adiponectin in Human Adipocytes and in Patients With Chronic Heart Failure

Osamu Tsukamoto, MD, PHD,*‡ Masashi Fujita, MD, PHD,‡ Mahoto Kato, MD,* Satoru Yamazaki, PHD,* Yoshihiro Asano, MD, PHD,‡ Akiko Ogai, PHD,* Hidetoshi Okazaki, MD, PHD,* Mitsutoshi Asai, MD,‡ Yoko Nagamachi, BS,‡ Norikazu Maeda, MD, PHD,§ Yasunori Shintani, MD, PHD,‡ Tetsuo Minamino, MD, PHD,‡ Masanori Asakura, MD, PHD,* Ichiro Kishimoto, MD, PHD,† Tohru Funahashi, MD, PHD,§ Hitonobu Tomoike, MD, PHD,* Masafumi Kitakaze, MD, PHD*

Suita, Osaka, Japan

Objectives We investigated the functional relationship between natriuretic peptides and adiponectin by performing both experimental and clinical studies.

Background Natriuretic peptides are promising candidates for the treatment of congestive heart failure (CHF) because of their wide range of beneficial effects on the cardiovascular system. Adiponectin is a cytokine derived from adipose tissue with various cardiovascular-protective effects that has been reported to show a positive association with plasma brain natriuretic peptide (BNP) levels in patients with heart failure.

Methods The expression of adiponectin messenger ribonucleic acid (mRNA) and its secretion were examined after atrial natriuretic peptide (ANP) or BNP was added to primary cultures of human adipocytes in the presence or absence of HS142-1 (a functional type A guanylyl cyclase receptor antagonist). Changes of the plasma adiponectin level were determined in 30 patients with CHF who were randomized to receive intravenous ANP (0.025 μg/kg/min human ANP for 3 days, n = 15) or saline (n = 15).

Results Both ANP and BNP dose-dependently enhanced the expression of adiponectin mRNA and its secretion, whereas such enhancement was inhibited by pre-treatment with HS142-1. The plasma adiponectin level was increased at 4 days after administration of human ANP compared with the baseline value (from 6.56 ± 0.40 μg/ml to 7.34 ± 0.47 μg/ml, $p < 0.05$), whereas there was no change of adiponectin in the saline group (from 6.53 ± 0.57 μg/ml to 6.55 ± 0.56 μg/ml).

Conclusions Natriuretic peptides enhance adiponectin production by human adipocytes in vitro and even in patients with CHF, which might have a beneficial effect on cardiomyocytes in patients receiving recombinant natriuretic peptide therapy for heart failure. (J Am Coll Cardiol 2009;53:2070–7) © 2009 by the American College of Cardiology Foundation

Plasma natriuretic peptide levels are increased in patients with congestive heart failure (CHF), and the measurement of these peptides is used widely to assess the presence, severity, and prognosis of CHF (1,2). Both atrial natriuretic peptide and brain natriuretic peptide (ANP and BNP, respectively) have a beneficial effect in patients with heart failure because of their various biological actions (3–5).

See page 2078

Adiponectin is a circulating cytokine derived from adipose tissue that has attracted considerable interest because of its identification as a risk factor for cardiovascular disease (6,7) and CHF (8). Adiponectin production is down-regulated in patients with coronary risk factors that are associated with the development of heart failure (9,10).

From the Cardiovascular Division of *Medicine and †Biochemistry, National Cardiovascular Center, Suita, Osaka, Japan; and the Departments of ‡Cardiovascular Medicine and §Metabolic Medicine, Osaka University Graduate School of Medicine, Suita, Osaka, Japan. This work is supported by grants-in-aid from the Ministry of Health, Labor, and Welfare-Japan, grants-in-aid from the Ministry of Education, Culture, Sports, Science and Technology-Japan, grants from the Japan Heart Foundation, and grants from the Japan Cardiovascular Research Foundation (all to Dr. Kitakaze) and Takeda Medical Research Foundation (to Dr. Funahashi). Drs. Tsukamoto, Fujita, and Kato contributed equally to this work.

Manuscript received August 27, 2008; revised manuscript received January 22, 2009, accepted February 19, 2009.

Recently, adiponectin was reported to have a cardioprotective effect against ischemia-reperfusion injury (11) and hemodynamic stress (12,13) in mice. Interestingly, it has been reported that the level of N-terminal pro-brain natriuretic peptide shows a positive correlation with the plasma adiponectin concentration in patients with chronic heart failure (14).

Given these experimental and clinical observations, we hypothesized that natriuretic peptides might increase adiponectin production in patients with heart failure to protect the cardiovascular system. Accordingly, in the present study, we investigated whether natriuretic peptides could directly increase adiponectin production by these adipocytes (and the cellular mechanisms involved) and confirmed this effect on adiponectin in the clinical setting.

Abbreviations and Acronyms

ANP = atrial natriuretic peptide
BNP = brain natriuretic peptide
CHF = congestive heart failure
GC-A = type A guanylyl cyclase receptor
hANP = human atrial natriuretic peptide
NPR = natriuretic peptide receptor
PKG = protein kinase G

Methods

Agents. Both human ANP and BNP were purchased from Sigma-Aldrich (St. Louis, Missouri). HS142-1, a functional guanylyl cyclase-A type receptor antagonist, was provided by Kyowa Hakko Kogyo Co., Ltd. (Mishima, Japan). A cGMP analog (8-pCPT-cGMP) and a selective cGMP-dependent protein kinase G (PKG) inhibitor (R_p-8-Br-PET-cGMP-S) were obtained from Biolog Life Science Institute (Bremen, Germany). An antibody directed against mouse adiponectin (MAB3608) was purchased from Chemicon International, Inc.

Primary culture and in vitro study of human adipocytes. Subcutaneous adipocytes derived from the adipose tissue of 6 women were obtained commercially together with culture medium from Zen-Bio, Inc. (Research Triangle Park, North Carolina. The donors were nonsmokers with a mean body mass index of 27.0 kg/m^2 (range 25.9 to 29.1 kg/m^2) and an average age of 47 years (range 29 to 63 years). Cells were maintained in adipocytes maintenance medium (i.e., AM-1) containing Dulbecco's modified Eagle medium/Ham's F-12 (1:1, v/v), 3% fetal calf serum, 15 mmol/l HEPES (pH 7.4), biotin, pantothenate, human insulin, 1 μmol/l dexamethasone, 100 U/ml penicillin, 100 μg/ml streptomycin, and 0.25 μg/ml amphotericin B at 37°C in a humidified atmosphere of 95% air/5% CO_2. The medium was changed every 2 days. Primary cultures of the adipocytes were used to examine the effects of natriuretic peptides (ANP or BNP) on the expression of adiponectin.

Before these experiments, the cells were plated in adipocyte basal medium (i.e., BM-1) containing Dulbecco's modified Eagle medium/Ham's F-12 (1:1, volume/volume), 15 mmol/l 4-(2-hydroxyethyl)-1-piperazineethanesulfonic acid (pH 7.4), biotin, and pantothenate for 24 h. Then the indicated concentrations of either natriuretic peptide (from 10^{-11} to 10^{-9} mol/l) were added to the BM-1 medium. After 24 h of incubation, the medium was harvested for Western blotting to measure the secretion of adiponectin, and the cells were also harvested for ribonucleic acid (RNA) analysis. The effect of each natriuretic peptide on adiponectin messenger ribonucleic acid (mRNA) levels was determined by quantitative real-time polymerase chain reaction (PCR).

Measurement of adiponectin. In patients with CHF, the plasma adiponectin concentration was measured by the use of an ELISA kit (Otsuka Pharmaceutical Co., Ltd., Tokyo, Japan) according to the manufacturer's protocol. Adiponectin secretion by primary cultured human adipocytes was assessed by Western blotting of the culture medium, as previously described (15), and the immunoreactive bands were quantified by densitometry (Molecular Dynamics, Sunnyvale, California).

Reverse transcriptional-PCR. Total RNA was extracted from adipocytes derived from human white fat with the use of RNA-Bee-RNA Isolation Reagent (Tel-Test, Inc., Gainesville, Florida). Then, 200 ng of total RNA was reversed transcribed and amplified by the use of an Omniscript RT kit (Qiagen, Hilden, Germany) according to the manufacturer's protocol. The forward primers for type A guanylyl cyclase receptor (GC-A) and natriuretic peptide receptor (NPR)-C were 5′-CCAGTTCCAAGTCTTTGCCAAGACAGCA and 5′-GGAAGACATCGTGCGCAATA, respectively, and the reverse primers for GC-A and NPR-C were 5′-CATTGTGTAGAAACAGCATGCCCTTGACGA and 5′-TGCTCCGGATGGTGTCACT, respectively. As a positive control, we used the samples of human cardiac tissue under the protocol approved by the institutional review board of the National Cardiovascular Center (No. 14-18) (16).

Quantitative real-time PCR analysis. Quantitative real-time PCR was performed as described previously (17). Oligonucleotide primers and TaqMan probes for human adiponectin and glyceraldehyde 3-phosphate dehydrogenase were purchased from Applied Biosystems (Foster City, California).

Subjects and design of the clinical study. We prospectively studied 30 consecutive CHF patients who were admitted to the emergency department of the National Cardiovascular Center between April and July 2006. The exclusion criteria were as follows: age >80 years, cardiogenic shock or hypotension (systolic blood pressure <100 mm Hg), and renal failure (serum creatinine >2.0 mg/dl). This study was approved by the Committee on Human Investigation of the National Cardiovascular Center, and all patients who participated gave informed consent. The 30 patients were randomized to 2 groups, a human atrial natriuretic peptide (hANP) group consisting of 15 patients who received administration of hANP and a control group consisting of 15 patients who were administered saline. In the hANP group, from immediately after the diagnosis of

acute exacerbation of CHF, hANP (0.025 μg/kg/min) was infused intravenously for 3 days. The study protocol did not restrict or specify any other diagnostic or therapeutic strategies. Blood for measuring the plasma adiponectin level was sampled before and 1 and 7 days after finishing the administration of hANP or saline (days 1, 4, and 10, respectively) (Fig. 3A).

Statistical analysis. For analysis of differences between the various treatments of adipocytes, analysis of variance was performed, followed by the appropriate post-hoc test. The differences in adiponectin levels between days 1 and 4 in each group were tested with a paired *t* test. The changes in adiponectin levels from day 1 to 4 between ANP group and saline group was tested with an unpaired *t* test. Results are expressed as the mean ± SEM, and p values of <0.05 were considered significant.

Results

Effect of natriuretic peptides on the expression and secretion of adiponectin by primary cultured human adipocytes. First, we checked the expression of GC-A and NPR-C mRNA by using reverse transcriptional-PCR. As shown in Figure 1A, both GC-A and NPR-C mRNA was detectable in primary cultured human adipocytes. To investigate the effects of natriuretic peptides on the regulation of adiponectin production in adipocytes, we incubated primary cultured human adipocytes with recombinant ANP. When ANP was used at a concentration of 10^{-10} mol/l (pathological plasma concentration), it increased adiponectin mRNA expression after 6 h of incubation and reached a maximum after 12 h (Fig. 1B). Next, we incubated human adipocytes with ANP at the concentration of from 10^{-11} mol/l (normal plasma concentration) to 10^{-9} mol/l (pharmacological plasma concentrations) and demonstrated enhanced adiponectin mRNA expression and adiponectin secretion into the medium in a dose-dependent manner, whereas these changes were completely inhibited by pretreatment with HS142-1 (Figs. 1C and 1D). Incubation of adipocytes with BNP also increased the expression of adiponectin mRNA in a dose-dependent manner and this effect was completely blocked by pretreatment with HS142-1 (Figs. 1E and 1F).

Involvement of cGMP/PKG signaling in natriuretic peptide-induced synthesis of adiponectin. Because both ANP and BNP exert their biological effects by promoting cGMP production, to investigate the role of the GC-A/cGMP/PKG signaling pathway in adiponectin production, we measured the changes of cGMP in ANP-treated primary cultured human adipocytes. We found that incubation with ANP increased the cGMP level and that this effect was blunted by co-treatment with HS142-1 (data not shown). Next, we treated human adipocytes with the cGMP analog 8-pCPT-cGMP and the PKG inhibitor (R_p)-8-Br-PET-cGMP-S. The activation of PKG by 8-pCPT-cGMP (50 μmol/l for 12 h) produced an increase of adiponectin mRNA expression similar to that observed after incubation with ANP. The effect of ANP on adiponectin mRNA expression was abolished in the presence of (R_p)-8-Br-PET-cGMP-S (100 nmol/l) (Fig. 2A). Consistent with these findings, adiponectin secretion into the culture medium also was increased by stimulation of the cGMP/PKG-dependent pathway (Fig. 2B). These results suggested that natriuretic peptides promote adiponectin synthesis via the GC-A/cGMP/PKG-dependent pathway.

Increase of plasma adiponectin levels in CHF patients treated with hANP. To confirm the effect of natriuretic peptides on the production of adiponectin, we conducted the clinical study. Thirty consecutive patients who met the inclusion criteria were enrolled in this clinical study. Fifteen patients were randomized to the ANP group, and 15 were assigned to the saline group. Baseline variables and treatments of the 2 groups are shown in Table 1. There were no differences in baseline clinical characteristics, hemodynamics, biochemical data, or medications. There was also no significant difference in the baseline plasma level of adiponectin between the 2 groups. As shown in Figure 3B, the plasma level of adiponectin did not change throughout the study in the saline group. On the other hand, the plasma adiponectin level at 1 day after finishing the administration of hANP (day 4) was significantly increased compared with the baseline value (day 1) in the ANP group, and it returned to baseline by 7 days after the completion of hANP infusion (day 10). These results suggested that hANP infusion led to an increase of the plasma adiponectin level in patients with CHF.

Discussion

In the present study, we demonstrated a novel effect of natriuretic peptides (ANP and BNP) on the production of adiponectin by adipocytes in both experimental and clinical studies. First, we clearly demonstrated that pathophysiological and pharmacological concentrations of either ANP or BNP increased adiponectin synthesis by primary cultured human adipocytes. Second, we showed that administration of recombinant ANP increased the plasma adiponectin level in patients with CHF.

ANP and BNP play an important role in the regulation of cardiovascular homeostasis. Their actions are primarily mediated via GC-A, which is expressed in various tissues and organs, including the kidneys, blood vessels, adrenal glands, and heart (18). Consistent with a previous report (19), we demonstrated that GC-A and NPR-C are expressed by human adipocytes. In the present study, we demonstrated a novel effect of both ANP and BNP on primary cultured human adipocytes, which was that pathophysiological or pharmacological concentrations of both peptides augmented adiponectin production by human adipocytes, with this effect being inhibited by treatment with HS142-1. Furthermore, we demonstrated that natriuretic peptides augment the production of adiponectin via a cGMP-dependent

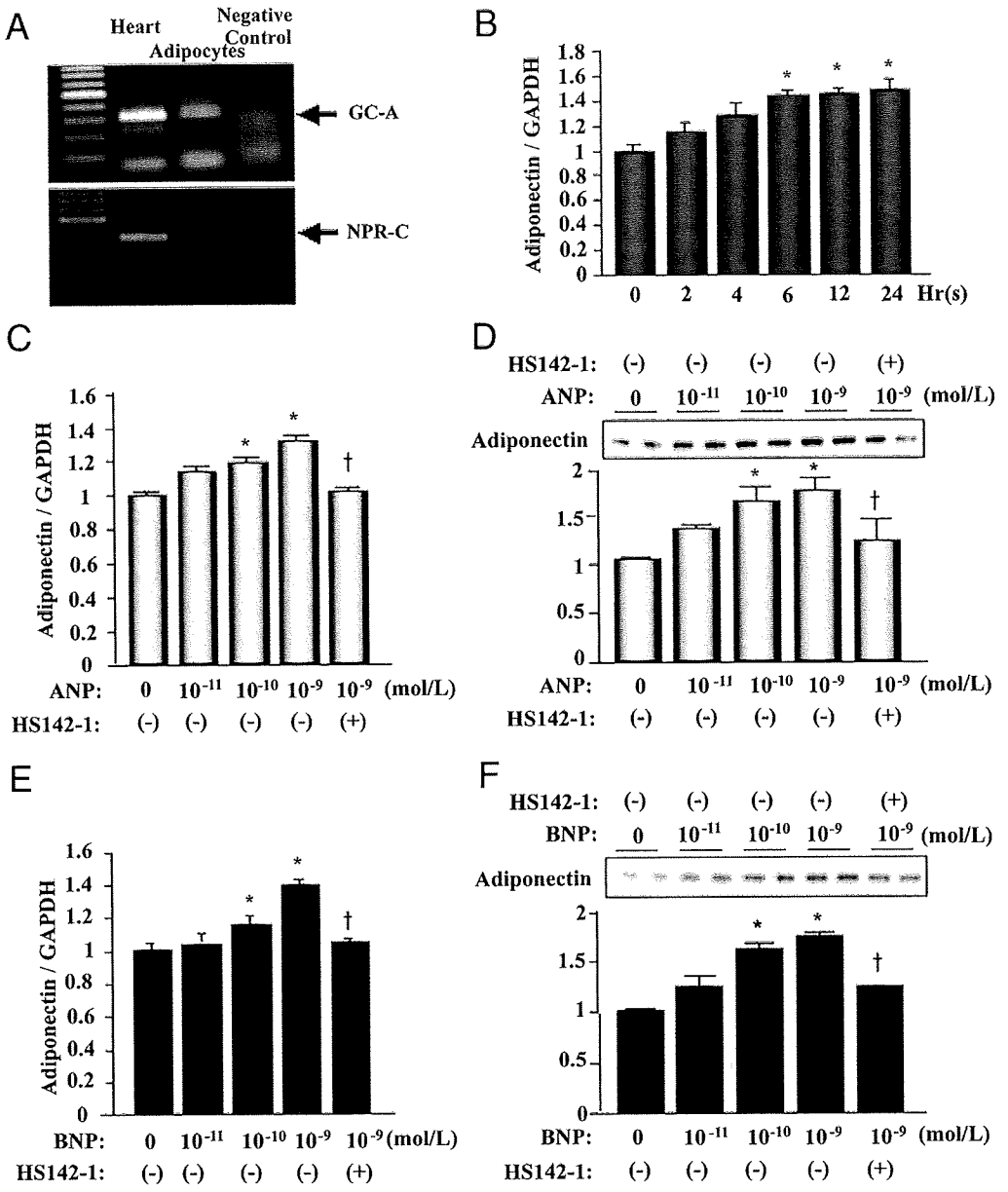

Figure 1 Effect of Natriuretic Peptides on the Expression and Secretion of Adiponectin by Primary Human Adipocytes

(A) Expression of GC-A receptors **(top)** and NPR-C **(bottom)** mRNA by primary cultured human adipocytes. Reverse-transcription PCR revealed expression of both GC-A receptors and NPR-C by human adipocytes. **(B)** Effect of ANP (10^{-10} mol/l) on the expression of adiponectin mRNA as determined by quantitative real-time PCR. **(C)** Dose-dependent effect of ANP on adiponectin mRNA expression, as determined by quantitative real-time PCR. Human adipocytes were treated with the indicated concentrations of ANP for 24 h. **(D)** Dose-dependent effect of ANP on adiponectin secretion into the culture medium. **(Top)** A representative Western blot of adiponectin. **(Bottom)** Quantitative analysis of adiponectin by densitometry. Values are normalized to the control. *$p < 0.05$ versus control, †$p < 0.05$ versus ANP 10^{-9} mol/l. **(E)** Dose-dependent effect of BNP on adiponectin mRNA expression, as determined by quantitative real-time PCR. **(F)** Dose-dependent effect of BNP on adiponectin secretion into the culture medium as determined by Western blotting. **(Top)** Representative Western blot of adiponectin. **(Bottom)** Quantitative analysis of adiponectin by densitometry. Values are normalized to the control. *$p < 0.05$ versus control. †$p < 0.05$ versus BNP 10^{-9} mol/l. ANP = atrial natriuretic peptide; BNP = brain natriuretic peptide; GC-A = type A guanylyl cyclase receptor; mRNA = messenger ribonucleic acid; NPR-C = natriuretic peptide receptor C; PCR = polymerase chain reaction.

pathway. These findings are important evidence that ANP and BNP regulate adiponectin production by human adipocytes.

Intravenous infusion of nesiritide (recombinant human BNP) has been reported to have beneficial hemodynamic effects in patients with CHF (4,5). The use of ANP also has been reported to have beneficial effects in patients with acute myocardial infarction (20,21). These beneficial effects have been attributed to the cardiovascular-protective actions of natriuretic peptides, including diuresis, natriuresis, vaso-

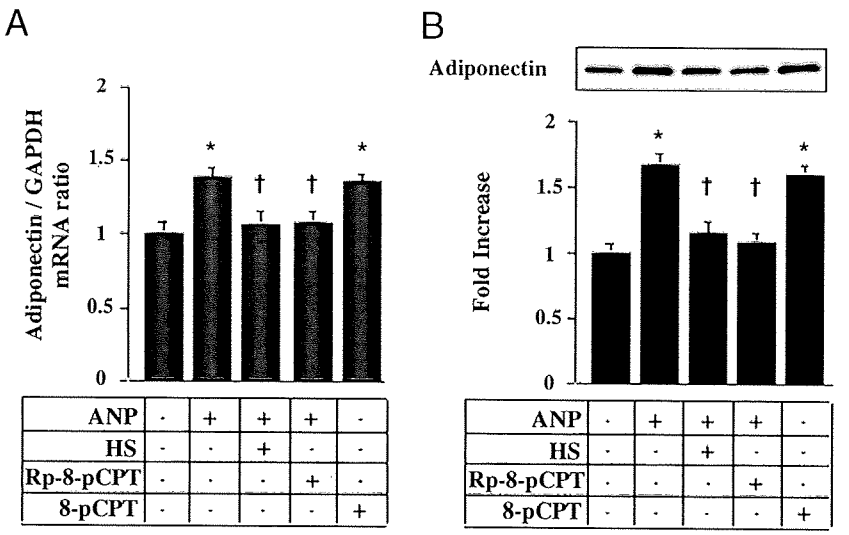

Figure 2 Involvement of the cGMP/PKG Signaling Pathway in the Induction of Adiponectin Synthesis by ANP

(A, B) Involvement of PKG was assessed by the treatment of primary cultured human adipocytes with 8-pCPT-cGMP (8-pCPT) and (R_p)-8-Br-PET-cGMP-S (Rp-8-pCPT). Adiponectin mRNA levels were determined by quantitative real-time PCR **(A)** and secretion of adiponectin into the culture medium was determined by Western blotting. Quantitative analysis of adiponectin secretion into the culture medium was done by densitometry **(B)**. Values are normalized to the control. *$p < 0.05$ versus control. †$p < 0.05$ versus ANP. HS = HS142-1; other abbreviations as in Figure 1.

dilation, and reduction of activity of the sympathetic nervous system and the renin-angiotensin-aldosterone system (3–5). In the present study, we administered recombinant ANP to patients with CHF and observed the changes of plasma adiponectin. The plasma adiponectin level of the ANP group was increased at 1 day after the finish of ANP administration compared with that in the control group, and then returned to baseline by 7 days after the completion of administration in patients with CHF.

Importantly, Moro et al. (22) showed that ANP did not affect the secretion of adiponectin in human abdominal adipose tissue from overweight women. This result may appear contradict ours, but we believe that is not the case. First, the concentration of ANP they used (10^{-6} mol/l) in the experiment of cultured adipocytes was greater than our concentration. Second, our data that recombinant ANP increased the plasma adiponectin levels were drawn from patients with heart failure, whereas the data of Moro et al. (22) were from cultured fat tissues of overweight women who underwent plastic surgery. However, they also demonstrated the potential stimulatory effect of ANP on adiponectin production from human adipose tissue in the presence of

Table 1 Clinical Characteristics of the 2 Groups

	hANP Group (n = 15)	Saline Group (n = 15)	p Value
Age (yrs)	60 ± 19	59 ± 19	NS
Sex (male/female)	9/6	10/5	NS
Heart rate (beats/min)	62 ± 11	66 ± 7	NS
Body mass index (kg/m^2)	21.4 ± 1.1	21.1 ± 1.7	NS
Systolic blood pressure (mm Hg)	116 ± 9	113 ± 9	NS
Diastolic blood pressure (mm Hg)	76 ± 12	74 ± 6	NS
NYHA functional class (II/III)	14/1	10/5	NS
LVEF by echocardiography (%)	32 ± 2	31 ± 8	NS
Plasma BNP (pg/ml)	506 ± 39	537 ± 33	NS
Other medications n (%)			
Loop diuretics	9 (60)	10 (67)	NS
Spironolactone	5 (33)	8 (53)	NS
ACEI or ARB	12 (80)	11 (80)	NS
Beta-blockers	13 (86)	12 (80)	NS

ACEI = angiotensin-converting enzyme inhibitors; ARB = angiotensin II receptor blockers; BNP = brain natriuretic peptide; hANP = human atrial natriuretic peptide; LVEF = left ventricular ejection fraction; NS = not significant; NYHA = New York Heart Association.

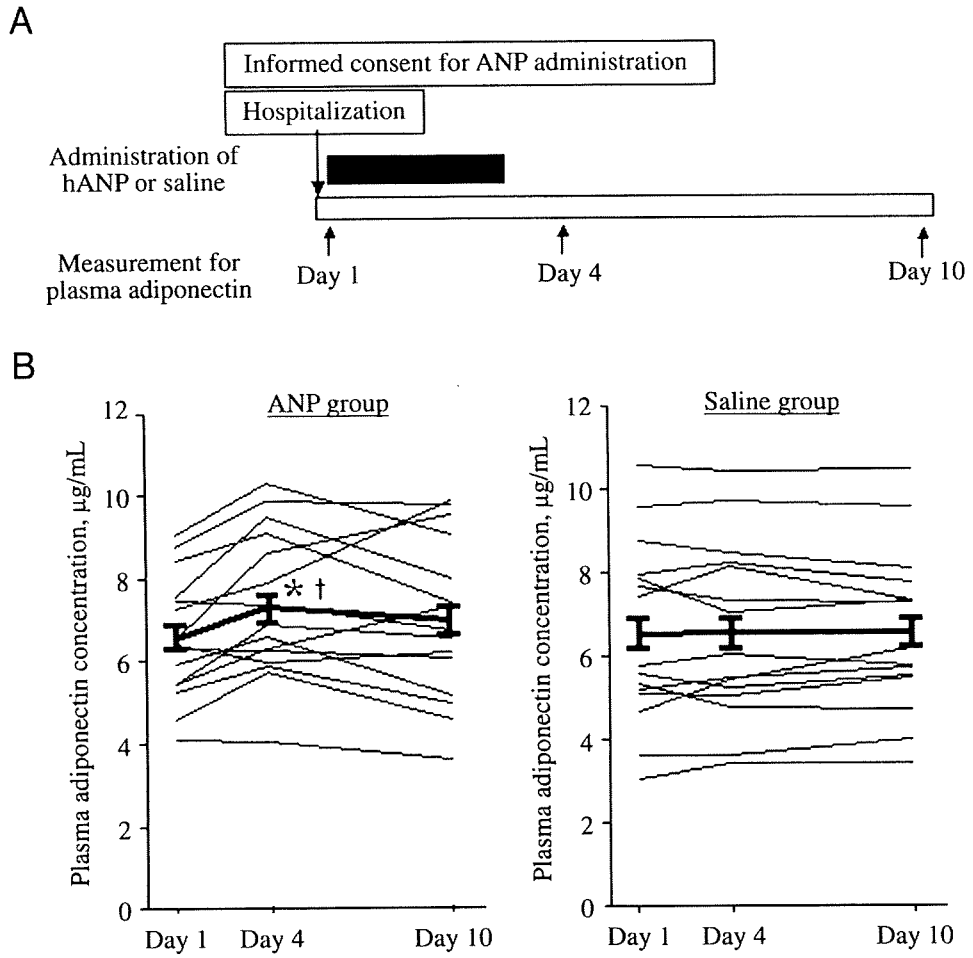

Figure 3 Increased Plasma Adiponectin Level in Patients With CHF After ANP Treatment

(A) Outline of the study protocol. hANP or saline was infused continuously for 3 days in the ANP and saline groups, respectively. The **black bar** indicates administration of either hANP (0.025 μg/kg/min) or saline. **(B)** The plasma adiponectin concentration profile after treatment in both groups. *$p < 0.05$ versus baseline in the ANP group; †$p < 0.05$ versus at the corresponding time in the saline group. CHF = congestive heart failure; hANP = human atrial natriuretic peptide; other abbreviations as in Figure 1.

hormone-sensitive lipase inhibitor, which inhibits the formation of lipolysis-derived byproducts by ANP-induced lipolysis (22).

Recently, Yu et al. (23) demonstrated the increased ANP-induced lipolysis rates in large adipocytes compared with small adipocytes. Thus, the difference of adipocyte size between patients with CHF and obesity might contribute to the different pattern of adiponectin secretion. Finally, catecholamines also are involved in the control of lipolysis in humans (24). Thus, the prolonged exposure of high plasma level of catecholamines or the treatment with beta-adrenergic receptor blockers in patients with CHF also might affect the distinct pattern of adiponectin secretion from adipocytes. Although precise mechanisms are unknown, the human adipocytes could secrete adiponectin when the certain stress was loaded. However, it remains possible that factors such as tumor necrosis factor-alpha (25) and alpha-adrenergic stimulation (26), both of which are increased in patients with CHF, may influence the expression of adiponectin or that adiponectin levels are affected by medical treatment, so further investigations are needed.

It is not clear whether ANP augments the plasma adiponectin levels in healthy subjects because of the ethical problems. However, we have reported that the plasma adiponectin level increased along with an increase of plasma BNP levels in 1,538 healthy subjects (27). These results suggest that an increase of natriuretic peptides augments the plasma adiponectin levels and exerts a cardioprotective effect in clinical settings.

Under normal conditions the adult heart utilizes predominantly fatty acids to derive the majority of its energy (28). However, metabolic remodeling such as a marked shift in substrate preference away from fatty acids toward glucose is observed in hypertrophic and failing hearts and the decrease

in fatty acid oxidation is not fully compensated for by an increase in glucose oxidation (29). Thus, the failing heart suffers from chronic energy starvation (30). Insulin resistance also is common in patients with heart failure (31). Adiponectin improves both glucose metabolism and insulin resistance via the AMPK signaling pathway (32). Therefore, we believe that the administration of recombinant natriuretic peptide has beneficial effects on cardiac energy metabolism via adiponectin in patients with CHF.

Interestingly, the plasma adiponectin level was reported to be decreased in patients with risk factors for heart failure (9,33–35) and increased along with BNP after the onset of heart failure (14). Although approximately 10% increase in adiponectin levels in the ANP group seems relatively small, this would not be the case because there was about a 20% reduction in plasma adiponectin levels in patients with coronary artery disease compared with those in control subjects (35), which leads us to believe that the 10% increase in adiponectin is important from the viewpoint of pathophysiology of heart diseases. Therefore, we hypothesized that ANP and/or BNP regulates the plasma level of adiponectin in patients with CHF and conducted this study.

Conclusions

We demonstrated that natriuretic peptides increase the production of adiponectin by human adipocytes, as well as in patients with CHF. These findings may help to shed more light on the pathophysiology of heart failure.

Acknowledgments

The authors thank Yukari Arino and Kieko Segawa for their secretarial work and Maki Miyoshi and Yoko Motomura for their excellent technical assistance.

Reprint requests and correspondence: Dr. Masafumi Kitakaze, Department of Cardiovascular Medicine, National Cardiovascular Center, Suita, Osaka 565-8565, Japan. E-mail: kitakaze@zf6.so-net.ne.jp.

REFERENCES

1. Maisel AS, Krishnaswamy P, Nowak RM, et al. Rapid measurement of B-type natriuretic peptide in the emergency diagnosis of heart failure. N Engl J Med 2002;347:161–7.
2. Stanek B, Frey B, Hulsmann M, et al. Prognostic evaluation of neurohumoral plasma levels before and during beta-blocker therapy in advanced left ventricular dysfunction. J Am Coll Cardiol 2001;38:436–42.
3. Levin ER, Gardner DG, Samson WK. Natriuretic peptides. N Engl J Med 1998;339:321–8.
4. Mills RM, LeJemtel TH, Horton DP, et al. Sustained hemodynamic effects of an infusion of nesiritide (human b-type natriuretic peptide) in heart failure: a randomized, double-blind, placebo-controlled clinical trial. Natrecor Study Group. J Am Coll Cardiol 1999;34:155–62.
5. Colucci WS, Elkayam U, Horton DP, et al. Intravenous nesiritide, a natriuretic peptide, in the treatment of decompensated congestive heart failure. Nesiritide Study Group. N Engl J Med 2000;343:246–53.
6. Lakka HM, Laaksonen DE, Lakka TA, et al. The metabolic syndrome and total and cardiovascular disease mortality in middle-aged men. JAMA 2002;288:2709–16.
7. Ninomiya JK, L'Italien G, Criqui MH, Whyte JL, Gamst A, Chen RS. Association of the metabolic syndrome with history of myocardial infarction and stroke in the Third National Health and Nutrition Examination Survey. Circulation 2004;109:42–6.
8. Ingelsson E, Sundstrom J, Arnlov J, Zethelius B, Lind L. Insulin resistance and risk of congestive heart failure. JAMA 2005;294:334–41.
9. Kenchaiah S, Evans JC, Levy D, et al. Obesity and the risk of heart failure. N Engl J Med 2002;347:305–13.
10. Hunt SA, Baker DW, Chin MH, et al. ACC/AHA guidelines for the evaluation and management of chronic heart failure in the adult: executive summary: a report of the American College of Cardiology/American Heart Association Task Force on Practice Guidelines (Committee to Revise the 1995 Guidelines for the Evaluation and Management of Heart Failure). J Am Coll Cardiol 2001;38:2101–13.
11. Shibata R, Sato K, Pimentel DR, et al. Adiponectin protects against myocardial ischemia-reperfusion injury through AMPK- and COX-2-dependent mechanisms. Nat Med 2005;11:1096–103.
12. Shibata R, Ouchi N, Ito M, et al. Adiponectin-mediated modulation of hypertrophic signals in the heart. Nat Med 2004;10:1384–9.
13. Liao Y, Takashima S, Maeda N, et al. Exacerbation of heart failure in adiponectin-deficient mice due to impaired regulation of AMPK and glucose metabolism. Cardiovasc Res 2005;67:705–13.
14. Kistorp C, Faber J, Galatius S, et al. Plasma adiponectin, body mass index, and mortality in patients with chronic heart failure. Circulation 2005;112:1756–62.
15. Maeda N, Takahashi M, Funahashi T, et al. PPARgamma ligands increase expression and plasma concentrations of adiponectin, an adipose-derived protein. Diabetes 2001;50:2094–9.
16. Okada K, Minamino T, Tsukamoto Y, et al. Prolonged endoplasmic reticulum stress in hypertrophic and failing heart after aortic constriction: possible contribution of endoplasmic reticulum stress to cardiac myocyte apoptosis. Circulation 2004;110:705–12.
17. Tsukamoto O, Minamino T, Okada K, et al. Depression of proteasome activities during the progression of cardiac dysfunction in pressure-overloaded heart of mice. Biochem Biophys Res Commun 2006;340:1125–33.
18. Nakao K, Ogawa Y, Suga S, Imura H. Molecular biology and biochemistry of the natriuretic peptide system. II: Natriuretic peptide receptors. J Hypertens 1992;10:1111–4.
19. Sengenes C, Zakaroff-Girard A, Moulin A, et al. Natriuretic peptide-dependent lipolysis in fat cells is a primate specificity. Am J Physiol Regul Integr Comp Physiol 2002;283:R257–65.
20. Kitakaze M, Asakura M, Kim J, et al. Human atrial natriuretic peptide and nicorandil as adjuncts to reperfusion treatment for acute myocardial infarction (J-WIND): two randomised trials. Lancet 2007;370:1483–93.
21. Hayashi M, Tsutamoto T, Wada A, et al. Intravenous atrial natriuretic peptide prevents left ventricular remodeling in patients with first anterior acute myocardial infarction. J Am Coll Cardiol 2001;37:1820–6.
22. Moro C, Klimcakova E, Lolmede K, et al. Atrial natriuretic peptide inhibits the production of adipokines and cytokines linked to inflammation and insulin resistance in human subcutaneous adipose tissue. Diabetologia 2007;50:1038–47.
23. Yu J, Yu HC, Kim KA, et al. Differences in the amount of lipolysis induced by atrial natriuretic peptide in small and large adipocytes. J Pept Sci 2008;14:972–7.
24. Moro C, Galitzky J, Sengenes C, Crampes F, Lafontan M, Berlan M. Functional and pharmacological characterization of the natriuretic peptide-dependent lipolytic pathway in human fat cells. J Pharmacol Exp Ther 2004;308:984–92.
25. Maeda N, Shimomura I, Kishida K, et al. Diet-induced insulin resistance in mice lacking adiponectin/ACRP30. Nat Med 2002;8:731–7.
26. Fasshauer M, Klein J, Neumann S, Eszlinger M, Paschke R. Adiponectin gene expression is inhibited by beta-adrenergic stimulation via protein kinase A in 3T3-L1 adipocytes. FEBS Lett 2001;507:142–6.

27. Ohara T, Kim J, Asakura M, et al. Plasma adiponectin is associated with plasma brain natriuretic peptide and cardiac function in healthy subjects. Hypertens Res 2008;31:825–31.
28. Makinde AO, Gamble J, Lopaschuk GD. Upregulation of 5′-AMP-activated protein kinase is responsible for the increase in myocardial fatty acid oxidation rates following birth in the newborn rabbit. Circ Res 1997;80:482–9.
29. van Bilsen M, Smeets PJ, Gilde AJ, van der Vusse GJ. Metabolic remodelling of the failing heart: the cardiac burn-out syndrome? Cardiovasc Res 2004;61:218–26.
30. Shen W, Asai K, Uechi M, et al. Progressive loss of myocardial ATP due to a loss of total purines during the development of heart failure in dogs: a compensatory role for the parallel loss of creatine. Circulation 1999;100:2113–8.
31. Swan JW, Anker SD, Walton C, et al. Insulin resistance in chronic heart failure: relation to severity and etiology of heart failure. J Am Coll Cardiol 1997;30:527–32.
32. Yamauchi T, Kamon J, Minokoshi Y, et al. Adiponectin stimulates glucose utilization and fatty-acid oxidation by activating AMP-activated protein kinase. Nat Med 2002;8:1288–95.
33. Della Mea P, Lupia M, Bandolin V, et al. Adiponectin, insulin resistance, and left ventricular structure in dipper and nondipper essential hypertensive patients. Am J Hypertens 2005;18:30–5.
34. Hotta K, Funahashi T, Arita Y, et al. Plasma concentrations of a novel, adipose-specific protein, adiponectin, in type 2 diabetic patients. Arterioscler Thromb Vasc Biol 2000;20:1595–9.
35. Kumada M, Kihara S, Sumitsuji S, et al. Association of hypoadiponectinemia with coronary artery disease in men. Arterioscler Thromb Vasc Biol 2003;23:85–9.

Key Words: adiponectin ■ natriuretic peptides ■ heart failure ■ adipose tissue.

Cardiovascular Research (2008) 79, 600–610
doi:10.1093/cvr/cvn128

EUROPEAN SOCIETY OF CARDIOLOGY®

Overexpression of endoplasmic reticulum-resident chaperone attenuates cardiomyocyte death induced by proteasome inhibition

Hai Ying Fu[1], Tetsuo Minamino[2]*, Osamu Tsukamoto[2], Tamaki Sawada[2], Mitsutoshi Asai[2], Hisakazu Kato[2], Yoshihiro Asano[2], Masashi Fujita[2], Seiji Takashima[2], Masatsugu Hori[2], and Masafumi Kitakaze[1]

[1]Department of Cardiovascular Medicine, National Cardiovascular Center, Suita, Osaka 565-8565, Japan; and [2]Department of Cardiovascular Medicine, Osaka University Graduate School of Medicine, 2-2 Yamadaoka, Suita, Osaka 565-0871, Japan

Received 17 December 2007; revised 8 April 2008; accepted 13 May 2008; online publish-ahead-of-print 28 May 2008

Time for primary review: 28 days

KEYWORDS
ER stress;
CHOP;
GRP78;
Proteasome inhibition;
Cardiomyocyte

Aims Proteasome inhibitors are a novel class of anticancer agents that induce tumour cell death via endoplasmic reticulum (ER) stress. Since ER stress is involved in the development of heart failure, we investigated the role of ER-initiated cardiomyocyte death by proteasome inhibition.
Methods and results Rat neonatal cardiomyocytes were used in this study. Proteasome activity was assayed using proteasome peptidase substrates. Cell viability and apoptosis were measured by 3-(4,5-dimethylthiazol-2-yl)-2,5-diphenol tetrazolium bromide and flow cytometry, respectively. Western blot analysis, real-time polymerase chain reaction (PCR) and reverse transcriptional PCR were used to detect the expression of protein and messenger ribonucleic acid (RNA). The location of overexpressed glucose-regulated protein (GRP) 78 was observed by confocal fluorescence microscopy. Proteasome inhibition induced cardiomyocyte death and activated ER stress-induced transcriptional factor ATF6, but not XBP1 (X-box binding protein 1), without up-regulating ER chaperones. ER-initiated apoptosis signalling, including cytosine-cytosine-adenine-adenine-thymine enhancer-binding protein (C/EBP) homologous protein (CHOP), c-Jun-N-terminal kinase (JNK), and caspase-12, was activated by proteasome inhibition. Short interference RNA targeting CHOP, but not the blockage of caspase-12 or JNK pathway, attenuated cardiomyocyte death. Overexpression of GRP78 suppressed both CHOP expression and cardiomyocyte death by proteasome inhibition.
Conclusion These findings demonstrate that proteasome inhibition induces ER-initiated cardiomyocyte death via CHOP-dependent pathways without compensatory up-regulation of ER chaperones. Supplement and/or pharmacological induction of GRP78 can attenuate cardiac damage by proteasome inhibition.

1. Introduction

Endoplasmic reticulum (ER) is an organelle that participates in the folding of membrane and secretory proteins. The conditions or stresses that interfere with ER function are named ER stress.[1] There are two ER stress-induced transcriptional factors to up-regulate ER-resident chaperones that promote the folding of accumulated proteins in ER: activating transcription factor 6 (ATF6) and X-box binding protein 1 (XBP1). ATF6 is cleaved in response to ER stress and the cleaved ATF6 traffics to nuclei to induce the expression of ER-resident chaperone.[2] In addition, ER stress induces *XBP1* messenger ribonucleic acid (mRNA) splicing, producing a new spliced *XBP1* mRNA.[3] The spliced XBP1 protein and cleaved ATF6 cooperatively up-regulate the expression of ER-resident chaperones that reduce ER stress.[4] Another important pathway to cope with ER stress is the degradation of misfolded proteins by the ubiquitin-proteasome system.[5] It is therefore conceivable that treatment of cells with proteasome inhibitors causes accumulation of misfolded proteins and ER stress. When the overload of misfolded proteins is not resolved, cell apoptosis signals are initiated from ER. This effect is mediated by increased expression of the transcription factor cytosine-cytosine-adenine-adenine-thymine enhancer-binding protein (C/EBP) homologous protein (CHOP) and activation of caspase-12 and c-Jun-N-terminal kinase (JNK).[6–8]

Recently, the ubiquitin-proteasome system is reported to be involved in the growth and survival of cells and

* Corresponding author. Tel: +81 6 6879 3472; fax: +81 6 6879 3473.
E-mail address: minamino@medone.med.osaka-u.ac.jp

considered as an attractive therapeutic target.[9] Proteasome inhibitors are usually short peptides linked to a pharmacophore that reacts with the active site of proteasome.[10] Based on the pharmacophores, proteasome inhibitors can be divided into several groups: peptide aldehydes (e.g. MG132), peptide boronates (e.g. PS341), and peptide epooxyketones (e.g. epoxomicin).[11] Among these proteasome inhibitors, bortezomib (PS341) has been used as anticancer agent against haematological malignancy and solid tumours.[12] Recently, the treatment with bortezomib was reported to be associated with cardiac failure in patients with lung cancer and multiple myeloma.[13,14] Furthermore, we have found that the accumulation of ubiquitinated proteins in failing heart samples from humans demonstrated the impairment of proteasome function in failing hearts.[15] These findings led us to hypothesize that the proteasome inhibition could cause cardiomyocyte death via an ER-dependent pathway. To test this hypothesis, we checked the role of ER-initiated apoptotic signalling in cardiomyocyte death when proteasome activity was pharmacologically inhibited. Furthermore, we also investigated whether overexpression of ER-resident chaperone could rescue cardiac cell death by proteasome inhibition. In the present study, we used MG132 and epoxomicin, two typical proteasome inhibitors, to investigate the effect of proteasome inhibition on cardiomyocytes. We also used tunicamycin, an inhibitor of N-linked glycosylation, as an ER stress inducer without affecting proteasome activity.

2. Methods

2.1 Materials

MG132, epoxomicin, and tunicamycin were purchased from Sigma Chemical Co. (St Louis, MO, USA). The antibodies for CHOP, XBP1, ATF6, and actin were obtained from Santa Cruz Biotechnology (Santa Cruz, CA, USA). The antibodies for phospho-JNK and JNK were obtained from Cell Signaling Technology, Inc. (Danvers, MA, USA). The antibodies for caspase-12 and HP1α were obtained from Sigma Chemical Co., while those for Lys-Asp-Glu-Leu (KDEL) and glyceraldehyde-3-phosphate dehydrogenase (GAPDH) were obtained from Assay Designs, Inc. (Ann Arbor, MI, USA) and Millipore Co. (Billerica, MA, USA). Z-Ala-Thr-Ala-Asp (Z-ATAD) and SP600125 were purchased from BioVision Inc. (Mountain View, CA, USA) and Calbiochem (San Diego, CA, USA), respectively.

2.2 Preparation of neonatal rat cardiomyocytes

Primary cardiomyocyte cultures were prepared from neonatal rat hearts as described previously.[16] All procedures were in accordance with the guiding principles of Osaka University School of Medicine, Position of the American Heart Association on Research Animal Use, and the Guide for the Care and Use of Laboratory Animals published by the US National Institute of Health (NIH Publication No. 85-23, revised 1996).

2.3 Proteasome activity assay

Chymotrypsin-like activities of proteasome were assayed using the fluorogenic peptides Suc-Leu-Leu-Val-Tyr-7-amino-4-methylcoumarin (LLVY-AMC) (Biomol, Plymouth Meeting, PA, USA) according to the method reported previously.[15] Briefly, after the treatment with MG132 or epoxomicin for 30 min, cultured rat neonatal cardiomyocytes were harvested, lysed in proteasome buffer (10 mmol/L Tris–HCl, pH 7.5, 1 mmol/L ethylene diamine tetraacetic acid (EDTA), 2 mmol/L adenosine-5'-triphosphate, 20% glycerol, and 4 mmol/L dithiothreitol), and centrifuged at 13 000 g at 4°C for 10 min. Then the supernatant (20 μg of protein) was incubated with proteasome activity assay buffer (0.05 mol/L Tris–HCl, pH 8.0, 0.5 mmol/L EDTA, 40 μmol/L LLVY-AMC) for 1 h at 37°C. The reaction was stopped by adding 0.9 mL of cold water and placing the reaction mixture on ice for at least 10 min. Subsequently, the fluorescence of the solution was measured by Fluorescence Microplate Reader (Gemini XS; Molecular Devices, Sunnyvale, CA, USA) with excitation at 380 nm (Ex) and emission at 440 nm (Em). All readings were standardized relative to the fluorescence intensity of an equal volume of free 7-amino-4-methylcoumarin (Sigma) solution (40 μmol/L).

2.4 Caspase-12 activity assay

Caspase-12 activity was assayed using its substrate ATAD-7-amino-4-trifluoromethyl coumarin. Cell lysate aliquots were assayed by Fluorescence Microplate Reader (Gemini XS; Molecular Devices) with 400 nm excitation and 505 nm emission filter according to the manufacturer's protocol (BioVision).

2.5 3-(4,5-Dimethylthiazol-2-yl)-2,5-diphenol tetrazolium bromide assay

Cardiomyocytes were seeded at 3×10^4/well in 96-well plates. After MG132 administration at appropriate conditions, cell numbers were measured with a water-soluble tetrazolium reagent [WST-8; 2-(2-methoxy-4-nitrophenyl)-3-(4-nitrophenyl)-5-(2,4-disulfophenyl)-2H-tetrazolium, monosodium salt] (Dojindo Laboratories, Kumamoto, Japan) according to the manufacturer's instructions. Cell viability was expressed as a percentage of the control. The wavelengths used in this assay were 450 nm (sample) and 630 nm (reference).

2.6 Western blot analysis

Cardiomyocytes were lysed in the buffer (0.15 mmol/L, NaCl 0.05 mmol/L Tris–HCl, pH 7.2, 1% Triton X-100, 1% sodium deoxycholate, 0.1% SDS) containing a protease inhibitor cocktail (Nakarai Tesque, Kyoto, Japan). Electrophoresis, immunoblotting, and detection were done as described previously.[15]

2.7 Reverse transcriptional polymerase chain reaction

After rat cardiomyocytes were treated with the drugs for 6 h, *XBP1* mRNA splicing was assessed using reverse transcriptional polymerase chain reaction (PCR) method. The primers that spanned the splice site are designed as followed: forward, ACGAGAGAAAACTCATGG; reverse, ACAGGGTCCAACTTGTCC (*Figure 1D*). This pair of primers can detect both spliced and unspliced *XBP1* at the size of 290 and 264 bp, respectively. The primers for GAPDH are forward, CATCAACGACCCCTTCATTGACCTCAACTA;reverse,TCCACGATGCCAAAGTTGTCATGGATGACC. PCR products were resolved on a 2% agarose gel and viewed by UV illumination.

2.8 Real-time quantitative polymerase chain reaction

We obtained samples after the drug treatment and then they were prepared according to the Omniscript Reverse Transcription Handbook (QIAGEN Inc., Hilden, Germany). The rat primers and probes used for quantification of glucose-regulated protein (GRP) 78, GRP94, CHOP, and GAPDH were all designed according to the manufacturer's protocol (Applied Biosystems, Foster City, CA, USA. https://www.appliedbiosystems.com/). Real-time PCR was performed with an ABI PRISM 7000 Sequence Detection System

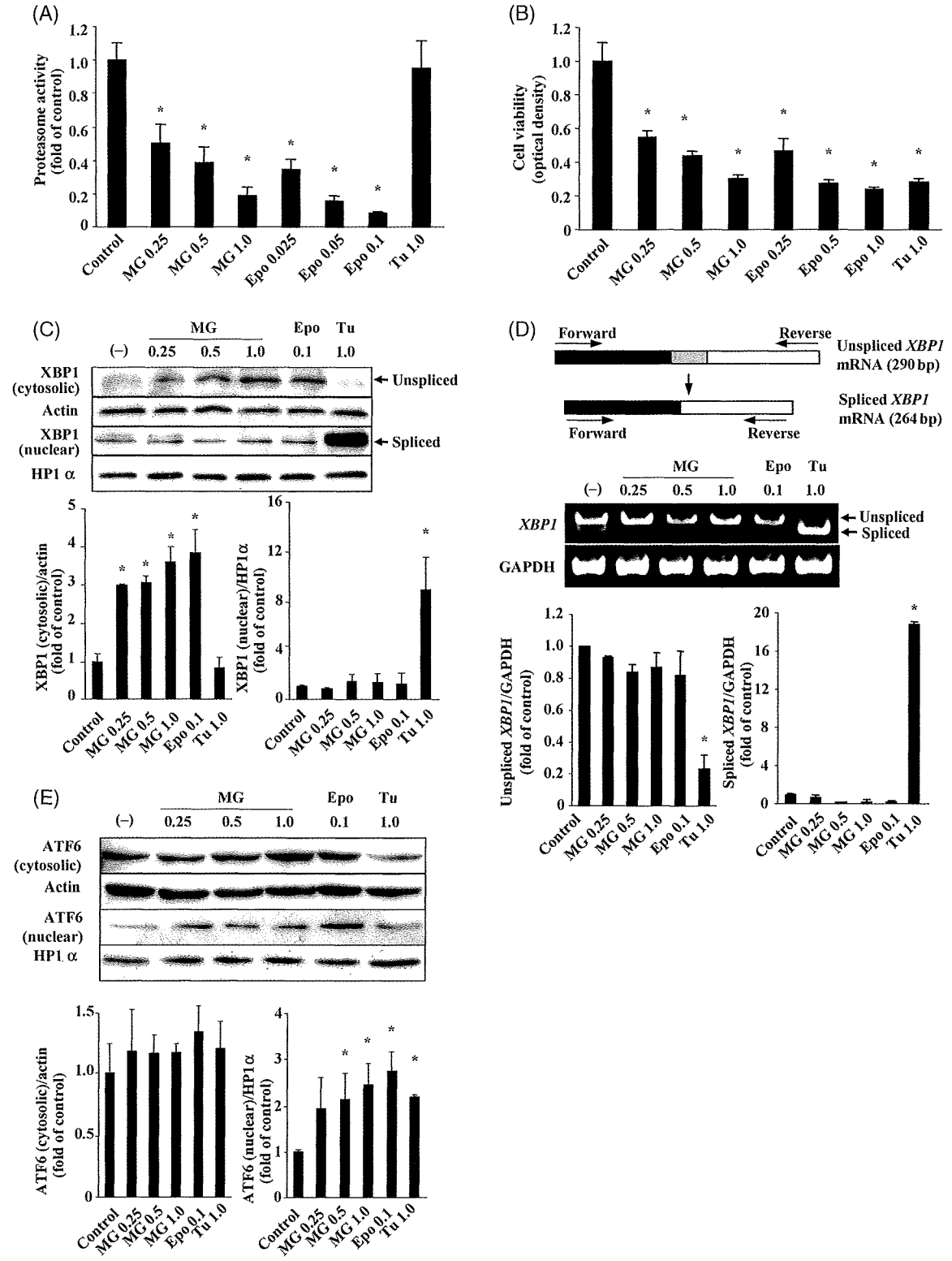

Figure 1 Effects of pharmacological proteasome inhibitors on the proteasome activity, cell death and endoplasmic reticulum stress-induced transcriptional factors in cultured cardiomyocytes. (*A*) Proteasome activity after the treatment with MG132 (MG) (0.25, 0.5, 1.0 μmol/L), epoxomicin (Epo) (0.025, 0.05, 0.1 μmol/L) or tunicamycin (Tu) (1.0 mg/mL) for 30 min. Experiments were repeated independently for three times ($n = 3$ in each experiment). (*B*) Cardiomyocyte viability after the treatment with MG, Epo or Tu for 48 h. Experiments were repeated independently for four times ($n = 6$ in each experiment). (*C*) Western blot analysis of spliced and unspliced X-box binding protein 1 (XBP1) proteins after the treatment with MG (0.25, 0.5, 1.0 μmol/L), Epo (0.1 μmol/L) or Tu (1.0 μg/mL) for 6 h. Actin and HP1α were used as the internal controls of cytosolic and nuclear fractions, respectively. (*D*) The upper panel shows the design of polymerase chain reaction (PCR) primers for *XBP1* messenger ribonucleic acid (mRNA) used in this study. This pair of primers can detect both unspliced and spliced *XBP1* mRNA. The middle and lower panels are representative and quantitative results of reverse transcriptional PCR for spliced and unspliced *XBP1* mRNA after the treatment with MG (0.25, 0.5, 1.0 μmol/L), Epo (0.1 μmol/L) or Tu (1.0 μg/mL) for 6 h. Glyceraldehyde-3-phosphate dehydrogenase was used as the internal control of mRNA expression. (*E*) Western blot analysis of ATF6 (activating transcription factor 6) in cytosolic and nuclear fractions after the treatment with MG (0.25, 0.5, 1.0 μmol/L), Epo (0.1 μmol/L) or Tu (1.0 μg/mL) for 6 h. The quantitative data in *C*, *D*, and *E* were achieved from three independent experiments. (Asterisk) $P < 0.05$ vs. control.

(Applied Biosystems) by the relative standard curve method. The thermal cycle reaction was performed as follows: 50°C for 2 min, 95°C for 10 min followed by 40 cycles at 95°C for 15 s, 60°C for 1 min. The target amount was determined from the relative standard curves constructed with serial dilutions of the control total cDNA.

2.9 Ribonucleic acid interference

We ordered four different short interfering ribonucleic acid (siRNA) from B-Bridge International, Inc. (Mountain View, CA, USA) to knock down CHOP mRNA (CHOP siRNA-1: 5′-CGAAGAGGAAGAAUCAAA-3′, siRNA-2: 5′-GGAAACAGCGACUGAAGGA-3′, siRNA-3: 5′-GGGACUGA GGGUAGACCAA-3′, siRNA-4: cocktail containing equal amounts of the above three types of siRNA). Rat cardiomyocytes were isolated and then incubated in Dulbecco's modified Eagle's medium (Invitrogen Co., Carlsbad, CA, USA). Opti-MEM (Invitrogen Co.), siRNA oligonucleotides (CHOP siRNA 1-4) (60 nmol/L) and Optifect (Invitrogen Co.) were added 4 h after cardiomyocyte isolation. As a negative control, cells were transfected with siRNA against firefly luciferase from Photinus pyralis (GL2 siRNA).

2.10 Flow cytometry

An Annexin V-fluorescein isothiocyanate (FITC) Apoptosis Detection Kit was purchased from Sigma. After the treatment of MG132, cardiomyocytes were washed twice with PBS and resuspended in binding buffer. FITC-Annexin V and propidium iodide were added according to the manufacturer's protocol. The mixture was incubated for 10 min in dark at room temperature and then cellular fluorescence was measured with a FACSscan flow cytometry (Becton, Dickinson and Company, Franklin Lakes, NJ, USA).

2.11 Adenovirus transduction

Recombinant adenovirus harbouring GRP78 gene was constructed as described previously,[17] and adenovirus harbouring LacZ was used as a control. Adenovirus was transfected 24 h after cardiomyocytes were isolated or 20 h after siRNA against CHOP was added. And the experiments were performed another 24 h after adenovirus infection.

2.12 Confocal fluorescence microscopy

Cardiomyocytes were observed by confocal microscopy (Radiance 2100 Laser Scanning System Bio-Rad, Hemei Hempstead, UK) and saved by LaserSharp 2000 (Bio-Rad). Alexa568 (red) (Invitrogen Co.) was scanned by helium/neon laser (wavelength 543 nm laser line) with long path 590 filter (560-700 nm excitation). Alexa488 (green) was captured by Argon laser (wavelength 488 nm laser line) with band path 500-550 IR filter (500-550 nm excitation). DAPI (blue) for nuclei staining of all cells was obtained in range of 400-470 nm excitation.

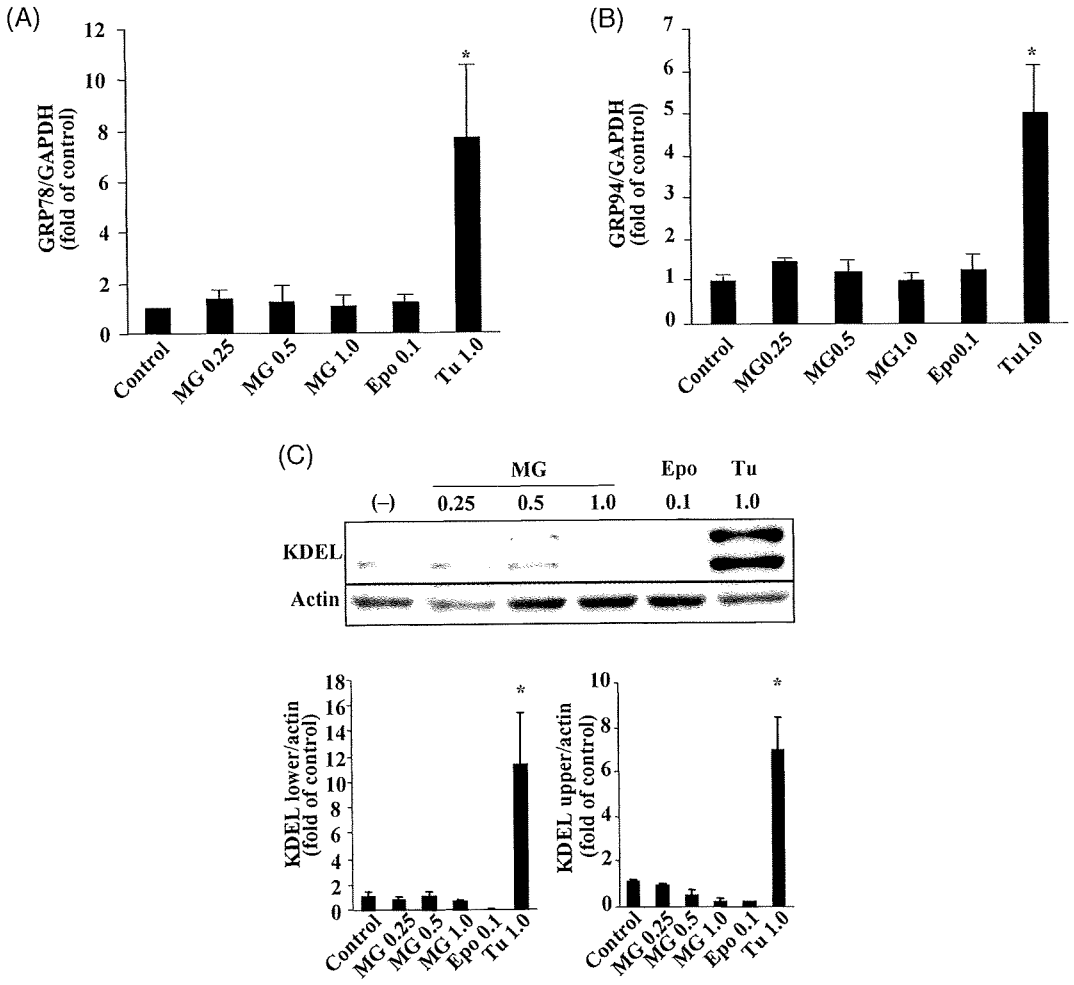

Figure 2 Endoplasmic reticulum chaperon expression by proteasome inhibition in cultured cardiomyocytes. Real-time polymerase chain reaction analysis of glucose-regulated protein (GRP) 78 (*A*) and GRP94 (*B*) ($n = 3$ in each experiment) and western blot analysis of Lys-Asp-Glu-Leu (KDEL) proteins (*C*) (upper and lower bands indicate GRP94 and GRP78, respectively) after the treatment with MG132 (MG) (0.25, 0.5, 1.0 μmol/L), epoxomicin (Epo) (0.1 μmol/L) or tunicamycin (Tu) (1.0 μg/mL) for 6 h. The western blot analysis and real-time PCR experiment were repeated for three times independently. (Asterisk) $P < 0.05$ vs. control.

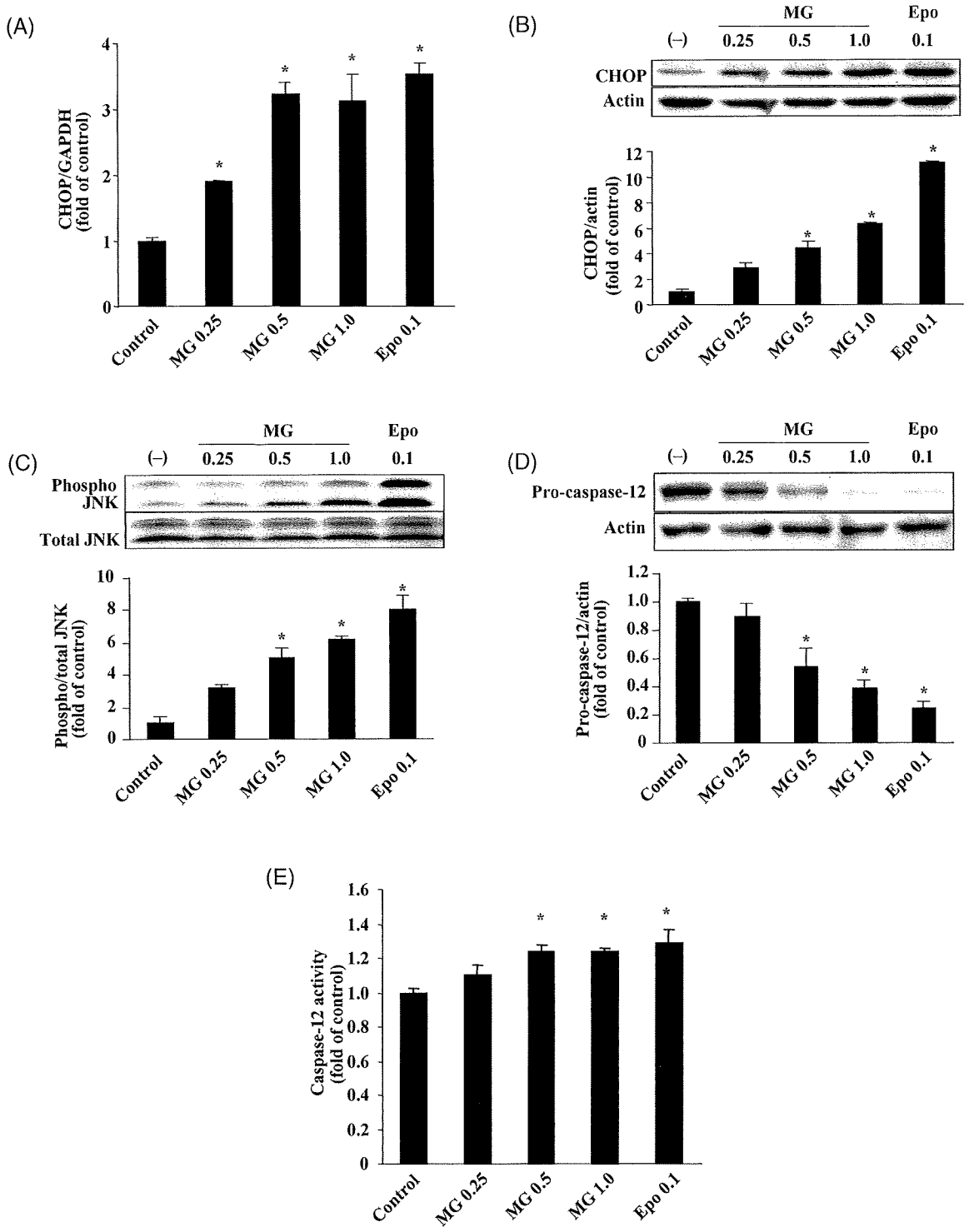

Figure 3 Activation of endoplasmic reticulum-initiated apoptosis signalling by proteasome inhibition in cultured cardiomyocytes. Real-time polymerase chain reaction (*A*) ($n = 3$ in each experiment) and western blot (*B*) analysis of CHOP [cytosine-cytosine-adenine-adenine-thymine (CCAAT) enhancer-binding protein (C/EBP) homologous protein] after the treatment with MG132 (MG) (0.25, 0.5, 1.0 μmol/L) or epoxomicin (Epo) (0.1 μmol/L) for 6 h. Western blot analysis of phospho-c-Jun-N-terminal kinase (JNK) (*C*) and pro-caspase-12 (*D*) after the treatment with MG (0.25, 0.5, 1.0 μmol/L) or Epo (0.1 μmol/L) for 1 and 6 h, respectively. (*E*) Caspase-12 activity after the treatment with MG (0.25, 0.5, 1.0 μmol/L) or Epo (0.1 μmol/L) for 6 h in cultured cardiomyocytes. Experiments were repeated independently for three times ($n = 3$ in each experiment). The quantitative data were achieved from three independent experiments. (Asterisk) $P < 0.05$ vs. control.

2.13 Statistical analysis

Data are expressed as the mean ± SEM. The results of cardiac proteasome activity, caspase-12 activity, cell viability and quantitative analysis of western blot analysis, real-time PCR, reverse transcription-PCR, and flow cytometry were compared by one-way factorial ANOVA followed by Bonferroni's correction. For all analyses, $P < 0.05$ was accepted as statistically significant.

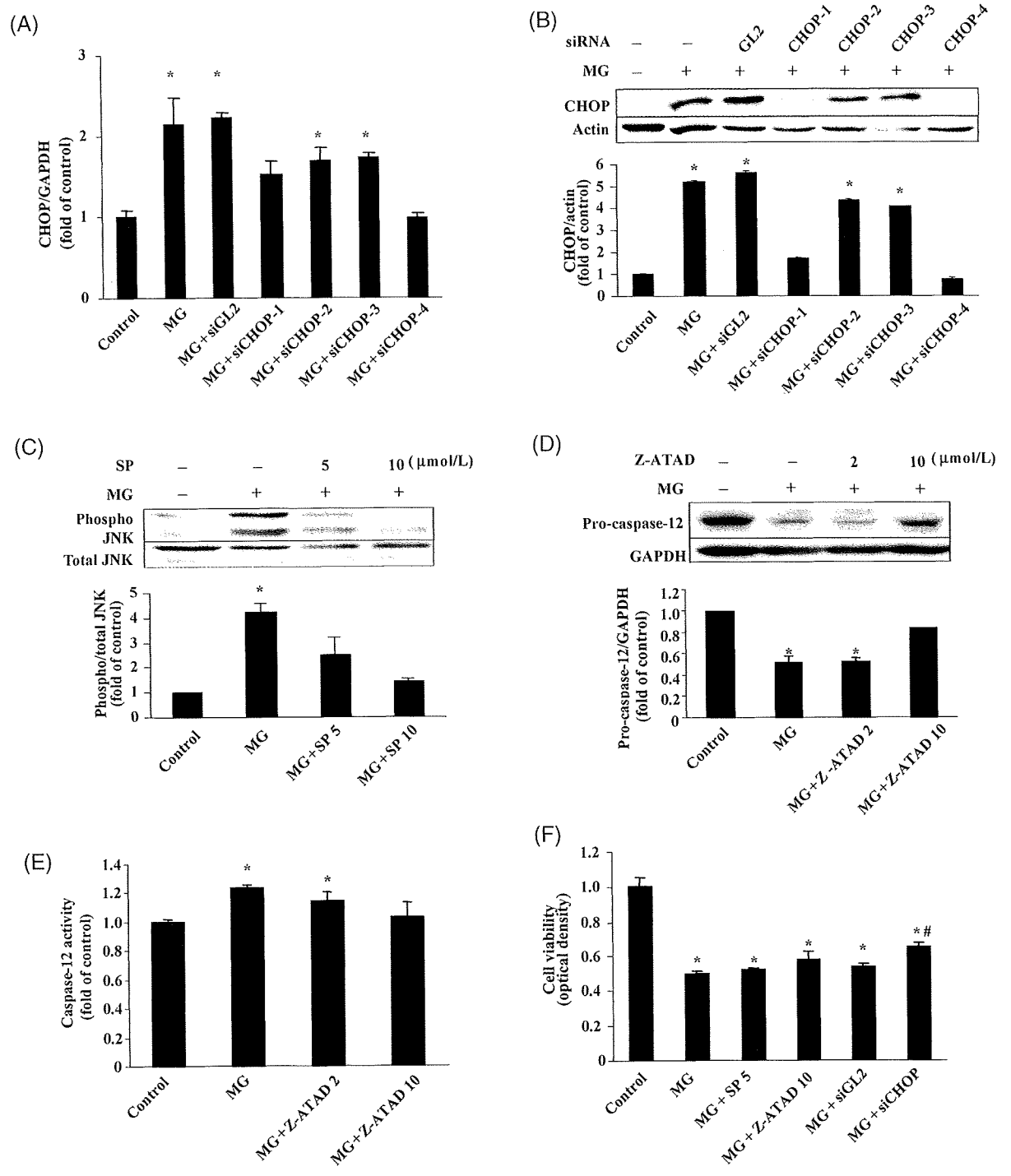

Figure 4 Effects of blockade of endoplasmic reticulum (ER)-initiated apoptosis signalling on apoptosis by proteasome inhibition in cultured cardiomyocytes. Effects of four different types of siRNA (short interfering ribonucleic acid) targeting CHOP [CCAAT enhancer-binding protein (C/EBP) homologous protein] on *CHOP* mRNA (*A*) ($n = 3$ in each experiment) and protein expression (*B*) after the treatment with MG132 (MG) (1.0 μmol/L) for 6 h. (*C*) Effects of SP600125 on JNK (c-Jun-N-terminal kinase) phosphorylation after the treatment with MG (1.0 μmol/L) for 1 h. SP600125 was added 1 h before MG (1.0 μmol/L) administration. (*D*) and (*E*) Effects of Z-Ala-Thr-Ala-Asp (Z-ATAD) on caspase-12 activation after the treatment with MG (1.0 μmol/L) for 6 h. Z-ATAD was added 1 h before MG (1.0 μmol/L) administration ($n = 3$ in each experiment). (*F*) Results of cardiomyocyte viability by MTT [3-(4,5-dimethylthiazol-2-yl)-2,5-diphenol tetrazolium bromide] assay after the co-treatment with MG (1.0 μmol/L) and blockers of ER-initiated apoptosis signals ($n = 6$ in each experiment). Representative (*G*) and quantitative (*H*) data of cardiomyocyte apoptosis by flow cytometry ($n = 3$ in each experiment). The population of cells in the lower right quadrant of dot plot indicated apoptotic cardiomyocytes. Results of western blot and flow cytometry analysis represented three independent experiments, while the result of cell viability was from four independent experiments, respectively. (Asterisk) $P < 0.05$ vs. control; (Hash) $P < 0.05$ vs. MG (1.0 μmol/L).